Development of a Numerical Framework for Modeling Fully Resolved Combustion Processes of Multiple Iron Particles

Moran Ezra, Oren Peles and Yoram Kozak
School of Mechanical Engineering, Tel Aviv University
Tel Aviv, Israel

1 Introduction

It is well-known that main reason for climate change is carbon dioxide (CO_2) emissions, mainly due to combustion of fossil fuels. Renewable energy sources, such as wind and solar, can potentially reduce carbon footprint. However, these energy sources are intermittent by nature, hence, energy storage solutions are necessary. One possible solution for energy storage is direct combustion of metal fuels in air [1]. The process of metal fuels' combustion is carbon free and in some cases, the combustion products, i.e. metal oxides, can be regenerated via renewable energy sources into metal, thus providing a fully sustainable cycle [2]. Iron is considered a promising metal fuel for direct combustion in atmospheric air since iron is the only metal, under these conditions, that burns heterogeneously due to its low vapor pressure [1]. Thus, for micro-metric sized iron particles, almost no iron-oxide nano-particles are produced and most of the iron-oxide products remain attached to the iron particle. This unique property allows collecting the micro-metric iron-oxide product particles as opposed to other metal fuels, where the oxide products are nano-sized. Moreover, iron is abundant on the Earth's crust and it is a very common industrial waste [3].

Various experimental and theoretical works investigated iron particle combustion in the past. Sun et al. [4] measured the burn time of micron-sized particles and developed a simple model that agreed with their experimental findings. Recently, new experimental results were presented by [5–7]. In their work, iron particles were carried by a gas and ignited using a laser beam. The thermal history of the particles was recorded via a thermal imaging camera. A recent theoretical work by Mi et al. [8] presented a numerical model for iron particle oxidation considering two oxide layers (FeO and Fe_3O_4). The model was also extended to take into account collective effects induced by multiple particles, which are known to affect ignition temperature and flame velocity [9].

However, as far as we know, currently, there is no numerical numerical framework that can fully resolve the flow field coupled with the ignition and combustion processes of multiple iron particles. For inert particles, such numerical frameworks exist, for example, Wang et al. [10] presented a numerical framework for calculating the heat transfer properties of inert agglomerates. By fully resolving the flow field around the particles, they have managed to derive simple correlations for particles' drag force and Nusselt number. Fully resolved simulations of aluminum particle combustion also exist, see, for instance [11–14].

Correspondence to: moranezra@mail.tau.ac.il

In this work, we present a high-fidelity numerical framework that can fully resolve the flow field around an arbitrary number of combusting iron particles. The framework is based on two separate solvers which are fully coupled. The first solver is a zero-dimensional (0-D) solver for iron particle combustion, and the second solver is our in-house Computational Fluid Dynamics (CFD) code for compressible flows - Athena-RFX++. Details about both of the solvers will be presented below, along with some preliminary results.

2 Numerical Framework

The following sections will describe the details regarding the numerical framework, including the CFD solver Athena-RFX++, the 0-D iron combustion model and the coupling strategy between both solvers.

2.1 Athena-RFX++ - CFD Solver

Athena-RFX++ is a fully compressible flow solver which is based on the open-source code - Athena++ [15]. The conservation equations are solved using a high-order Godunov method. In the case of iron particle combustion, we solve the Navier–Stokes equations with heat and mass transfer effects. Since the original open source code utilizes a perfectly structured grid, complex geometries cannot be modeled. Therefore, we implemented an Immersed Boundary Method (IBM) [16] in the code. In the IBM, the solid body is treated as an interface, where the boundary conditions are enforced in the fluid domain. For more details on the implemented IBM formulation see [17, 18]. During the CFD simulation, flow variables are calculated at the particle's wall and transferred to a 0-D model for iron particle combustion, which will be described in the following section.

2.2 Iron Particle Combustion - 0-D Solver

The 0-D solver for iron particle combustion is based on the following assumptions:

1. There are no temperature or concentration gradients within the particle.
2. There are two oxide layers, FeO and $\mathrm{Fe_3O_4}$, which remain attached to the Fe core.
3. Below melting temperature of the iron oxides, the combustion is controlled by internal diffusion processes of oxygen and Fe into the oxide layer
4. Above melting temperature of the iron oxides, the combustion is controlled by the external oxygen flux, from the ambient to the particle, through a boundary layer.
5. Evaporation of the iron and the iron oxides is negligible due to their low vapor pressure.
6. Thermal expansion is negligible.

To obtain the particle's temperature during the combustion process, the energy equation (Eq. 1) must be solved, see also [8]. The main heat sources in the equation are the heat release from the oxides formations (first and second terms at the right hand side of the equation) and the heat loss to the ambient, Q, by convection and radiation (see Eq. 2). The temperature dependent properties of the air, iron, FeO and $\mathrm{Fe_3O_4}$ were taken from [19] and NASA [20].

$$\frac{dH_p}{dt} = q_{FeO} \cdot \frac{dm_{FeO}}{dt} + q_{Fe_3O_4} \cdot \frac{dm_{Fe_3O_4}}{dt} - Q, \tag{1}$$

where H_p is the particle's enthalpy, q_{FeO} and $q_{Fe_3O_4}$ are the heat release from the oxides formation, and $\frac{dm_{FeO}}{dt}$ and $\frac{dm_{Fe_3O_4}}{dt}$ are the growth mass rates of the oxides.

$$Q = A_p h_p (T_p - T_\infty) + A_p \sigma \epsilon (T_p^4 - T_\infty^4), \tag{2}$$

where A_p is the surface area of the particle, h_p is the heat transfer coefficient, σ is the Stefan-Boltzmann constant, ϵ is the particle's emissivity, T_p is the particle's temperature and T_∞ is the ambient temperature.

Note that the 0-D model was previously validated against experimental data by [6] with good agreement, see [17]. The coupling strategy between the 0-D and the CFD solvers is described in detail below.

2.3 Coupling the Solvers

As presented above, we developed two separate solvers. These solvers are coupled using the following procedure:

1. The mass and heat fluxes are calculated at the particles' wall (Nusselt and Sherwood numbers) and transferred to the 0-D model.
2. The particle temperature is calculated using the 0-D solver and then it is enforced as a Dirichlet boundary condition at the particles' wall. In addition, the oxygen concentration is zero at the particle's wall, assuming external diffusion controlled process (see 0-D model assumptions).

As each solver is time-dependent, the coupled framework time step equals to the minimum time step of the two solvers. Typically, the time step of the 0-D model is greater than the time step of the CFD solver.

3 Results

In this section, we present, for the first time, as far as we know, fully coupled and resolved three-dimensional numerical simulations of iron particles' combustion in air. In particular, we examine a $3\times3\times3$ in-line arranged array of iron particles. The Reynolds number chosen for this simulation is 20 and the grid size is $192\times64\times64$ with 5 levels of refinement at the particles' surrounding (about 200M cells in total). The domain size is $60D\times40D\times40D$, where $D = 54$ μm is the particle diameter. The ambient air temperature is $\sim$1200 K and the pressure is 101000 Pa. The temperature and oxygen concentration contours are presented in Fig. 1 for 0.06 seconds after the simulation started. It can be seen that the air is heated due to the particles' combustion. Moreover, the oxygen concentration near the particles is significantly reduced due to the oxygen consumption by the chemical reactions at the particles' surface. The resulting flow field is complex, which leads to a unique combustion process for each particle.

In Fig. 2, the temperature history of several particles is presented. Qualitatively, for each particle, the combustion process is similar. It involves heating and melting, further temperature increase until the Fe core is fully consumed, and then a cooling process accompanied by the iron-oxide solidification. Nevertheless, the particle position leads to significant quantitative differences in the temperature history. For iron particles located further downstream, the combustion process is delayed. This is due to lower

oxygen concentration induced by oxygen consumption of iron particles found further upstream. Moreover, iron particles that are located downstream have higher maximum temperatures, due to the heated surrounding by the upstream iron particles. It is important to mention that the Nusselt and Sherwood numbers are changing over time due to the flow transients.

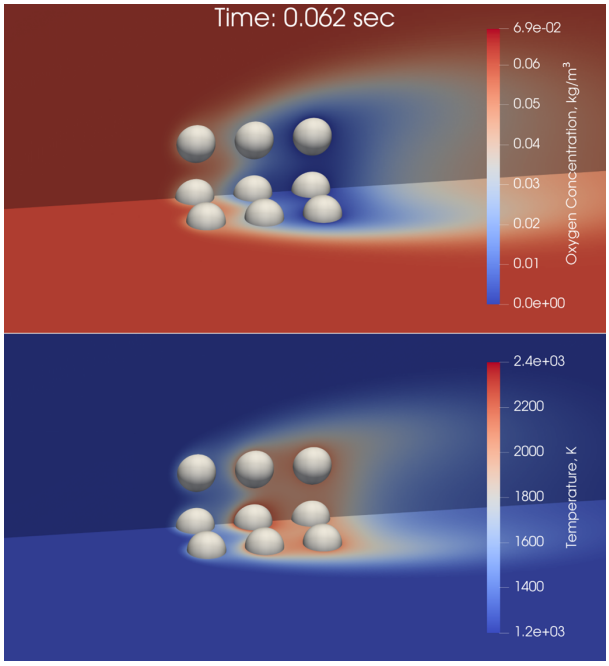

Figure 1: Combustion process of 27 inline iron particles in air, with a 54 micrometer diameter and Reynolds number of 20 - Oxygen concentration and temperature contours at 0.06 seconds.

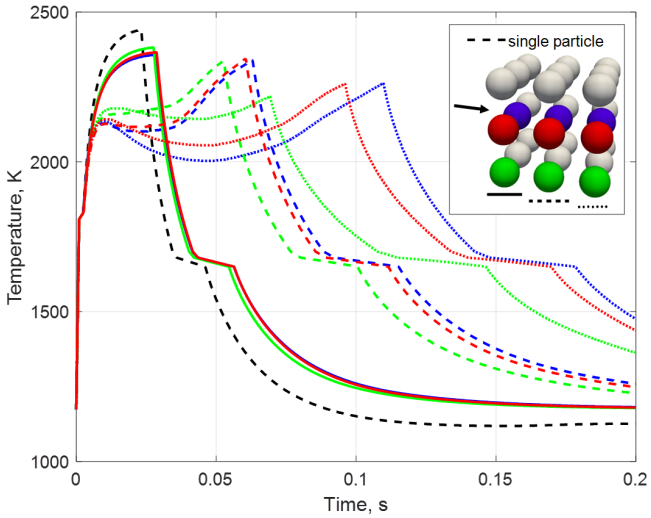

Figure 2: Combustion process of 27 inline iron particles in air, with a 54 micrometer diameter and Reynolds number of 20 - Thermal history of the particles. For comparison, a single particle thermal history is also presented.

4 Acknowledgments

We would like to thank the Israeli Ministry of Energy, PlanNetZero - Tel Aviv University Climate Crisis Initiative, and the Gordon Center for Energy Studies for supporting and funding this research.

References

[1] J. Bergthorson, S. Goroshin, M. Soo, P. Julien, J. Palecka, D. Frost, and D. Jarvis, "Direct combustion of recyclable metal fuels for zero-carbon heat and power," *Applied Energy*, vol. 160, pp. 368–382, 2015.

[2] J. M. Bergthorson, "Recyclable metal fuels for clean and compact zero-carbon power," *Progress in Energy and Combustion Science*, vol. 68, pp. 169–196, 2018.

[3] D. Wen, "Nanofuel as a potential secondary energy carrier," *Energy & Environmental Science*, vol. 3, no. 5, pp. 591–600, 2010.

[4] J.-H. Sun, R. Dobashi, and T. Hirano, "Combustion behavior of iron particles suspended in air," *Combustion Science and Technology*, vol. 150, no. 1-6, pp. 99–114, 1990.

[5] D. Ning, Y. Shoshin, J. A. van Oijen, G. Finotello, and L. de Goey, "Burn time and combustion regime of laser-ignited single iron particle," *Combustion and Flame*, vol. 230, p. 111424, 2021.

[6] D. Ning, Y. Shoshin, M. van Stiphout, J. van Oijen, G. Finotello, and P. de Goey, "Temperature and phase transitions of laser-ignited single iron particle," *Combustion and Flame*, vol. 236, p. 111801, 2022.

[7] S. Li, J. Huang, W. Weng, Y. Qian, X. Lu, M. Aldén, and Z. Li, "Ignition and combustion behavior of single micron-sized iron particle in hot gas flow," *Combustion and Flame*, vol. 241, p. 112099, 2022.

[8] X. Mi, A. Fujinawa, and J. M. Bergthorson, "A quantitative analysis of the ignition characteristics of fine iron particles," *Combustion and Flame*, vol. 240, p. 112011, 2022.

[9] M. Soo, X. Mi, S. Goroshin, A. J. Higgins, and J. M. Bergthorson, "Combustion of particles, agglomerates, and suspensions–a basic thermophysical analysis," *Combustion and Flame*, vol. 192, pp. 384–400, 2018.

[10] F. Municchi and S. Radl, "Consistent closures for euler-lagrange models of bi-disperse gas-particle suspensions derived from particle-resolved direct numerical simulations," *International Journal of Heat and Mass Transfer*, vol. 111, pp. 171–190, 2017.

[11] M. Beckstead, Y. Liang, and K. Pudduppakkam, "Numerical simulation of single aluminum particle combustion," *Combustion, Explosion and Shock Waves*, vol. 41, pp. 622–638, 2005.

[12] R. W. Houim and K. K. Kuo, "A ghost fluid method for compressible reacting flows with phase change," *Journal of Computational Physics*, vol. 235, pp. 865–900, 2013.

[13] J. Glorian, S. Gallier, and L. Catoire, "On the role of heterogeneous reactions in aluminum combustion," *Combustion and Flame*, vol. 168, pp. 378–392, 2016.

[14] P. Das and H. Udaykumar, "Sharp-interface calculations of the vaporization rate of reacting aluminum droplets in shocked flows," *International Journal of Multiphase Flow*, vol. 134, p. 103442, 2021.

[15] J. M. Stone, K. Tomida, C. J. White, and K. G. Felker, "The athena++ adaptive mesh refinement framework: Design and magnetohydrodynamic solvers," *The Astrophysical Journal Supplement Series*, vol. 249, no. 1, p. 4, 2020.

[16] Y.-H. Tseng and J. H. Ferziger, "A ghost-cell immersed boundary method for flow in complex geometry," *Journal of Computational Physics*, vol. 192, no. 2, pp. 593–623, 2003.

[17] M. Ezra, O. Peles, and Y. Kozak, "Development of a high-fidelity numerical framework for fully resolving combustion of liquid iron droplets in air," in *ILASS–Europe 2022, 31th Conference on Liquid Atomization and Spray Systems*, 2022.

[18] M. Ezra and Y. Kozak, "Development of an immersed boundary method for high-speed compressible flows," in *AIAA SCITECH 2023 Forum*, p. 1401, 2023.

[19] M. W. Chase Jr, "Nist-janaf thermochemical tables," *J. Phys. Chem. Ref. Data, Monograph*, vol. 9, 1998.

[20] B. J. McBride, *Coefficients for calculating thermodynamic and transport properties of individual species*, vol. 4513. National Aeronautics and Space Administration, 1993.